Supplementary Material

Table S1. $^{13}C$ CP/MAS NMR structural parameters.

| Symbol | Carbon type | Structural Formula | Chemical shift (ppm) | RC (%) |
|---|---|---|---|---|
| $f_{al}^{*}$ | Terminal methyl group, lipomethyl group |  | 8~16<br>16~25 | 7.77 |
| $f_{al}^{H}$ | Methylidene, CH2 of saturated cyclic hydrocarbons | 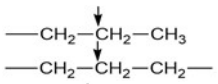 | 25~36<br>36~51 | 13.41 |
| $f_{al}^{O}$ | Fatty carbon associated with oxygen | 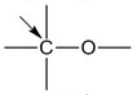 | 51~75<br>75~90 | 0.49 |
| $f_{a}^{H+B}$ | Protonated aryl carbon |  | 90~137 | 49.69 |
| $f_{a}^{H}$ | Aryl carbon with protons | 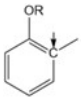 | 90~129 | 36.17 |
| $f_{a}^{N}$ | Aprotonated carbon | | 129~165 | 36.65 |
| $f_{a}^{B+S}$ | Aromatic carbon bonded to carbon |  | 129~150 | 26.34 |
| $f_{a}^{B}$ | Interaromatic ring bridge carbon, collateral aromatic carbon | 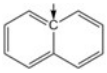 | 129~137 | 12.91 |
| $f_{a}^{S}$ | Alkyl groups replace aryl carbons | 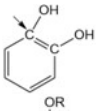 | 137~150 | 13.03 |
| $f_{a}^{P}$ | Methoxy-substituted aryl carbon | 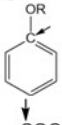 | 150~155<br>155~165 | 10.06 |
| $f_{a}^{C}$ | Carboxyl carbon |  | 165~188 | 4.53 |
| | Carbonyl carbon |  | 188~220 | |
| $f_{a}'$ | Aromatic carbon | - | 90-165 | 73.43 |

Table S2. O1s compositional analysis of RC.

| .. | O1s | | | |
|---|---|---|---|---|
| | 531.07eV | 532.21eV | 533.22eV | 534.12eV |
| | O=C-O | C=O | C-O-C | -OH |
| RC | 10.74 | 40.20 | 37.33 | 11.74 |

Table S3 Deconvoluted band assignments of Raman spectra.

| Sample | Band | Line Shape | $A_{D1}/A_G$ |
|---|---|---|---|
| CG0 | D1<br>G | Gauss | 3.31 |
| CG | D1<br>G | Gauss | 2.34 |
| CGNa0.1 | D1<br>G | Gauss | 2.25 |

Table S4 Relative contents of functional groups and $sp^2C/sp^3C$ ratio of CG0、CG、CGNa0.1 in the C 1s spectrum

| Sample | C 1s | | | | | |
|---|---|---|---|---|---|---|
| | 284.7 eV $sp^2$ C | 285.15 eV $sp^3$ C | 286.64 eV C-O | 289.0 eV C=O | 291.1 eV O=C-O | $sp^2/sp^3$ |
| CG0 | 40.63 | 40.84 | 10.56 | 4.87 | 3.11 | 0.99 |
| CG | 41.85 | 38.31 | 10.67 | 5.00 | 4.17 | 1.09 |
| CGNa0.1 | 42.72 | 38.94 | 9.92 | 4.21 | 4.20 | 1,10 |

Table S5 Relative contents of functional groups of CG0、CG、CGNa0.1 in the O1s spectrum

| Sample | O 1s | | | |
|---|---|---|---|---|
| | 531.42 eV O=C-O | 532.34 eV C=O | 533.51 eV C-O-C | 535.17 eV -OH |
| CG0 | 37.76 | 26.02 | 28.89 | - |
| CG | 34.17 | 28.43 | 32.08 | - |
| CGNa0.1 | 38.44 | 26.11 | 32.33 | - |

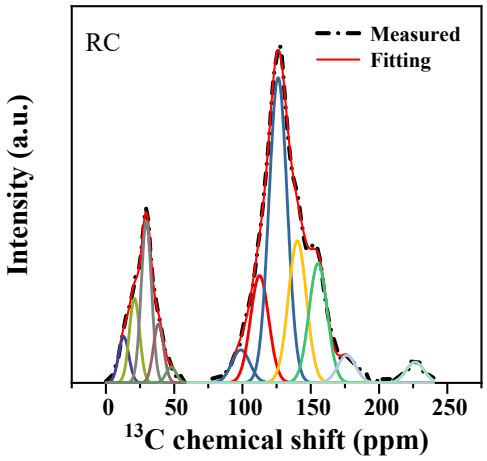


Figure S1. $^{13}C$ CP/MAS NMR peak-fitting curve of RC.

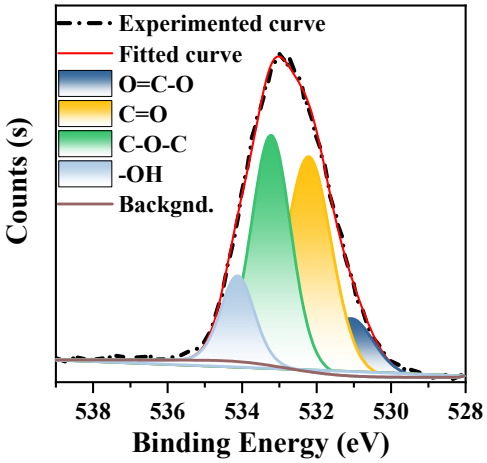


Figure S2. O1s spectra peak fitting of RC.

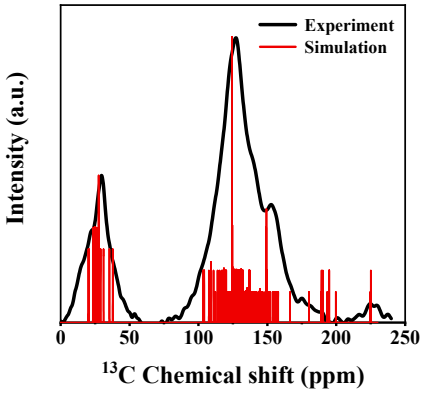


Figure S3. Experimental values and simulated maps of $^{13}C$ CP/MAS NMR.

Figure S4c indicates that the potential energies of the three structures have stabilized during the 200 ps simulation. In Figure S4d, the significant increase in pyrolysis fragments in the BCGNa0.1 sample further confirms the pronounced role of $Na_2CO_3$ in promoting coal pyrolysis.

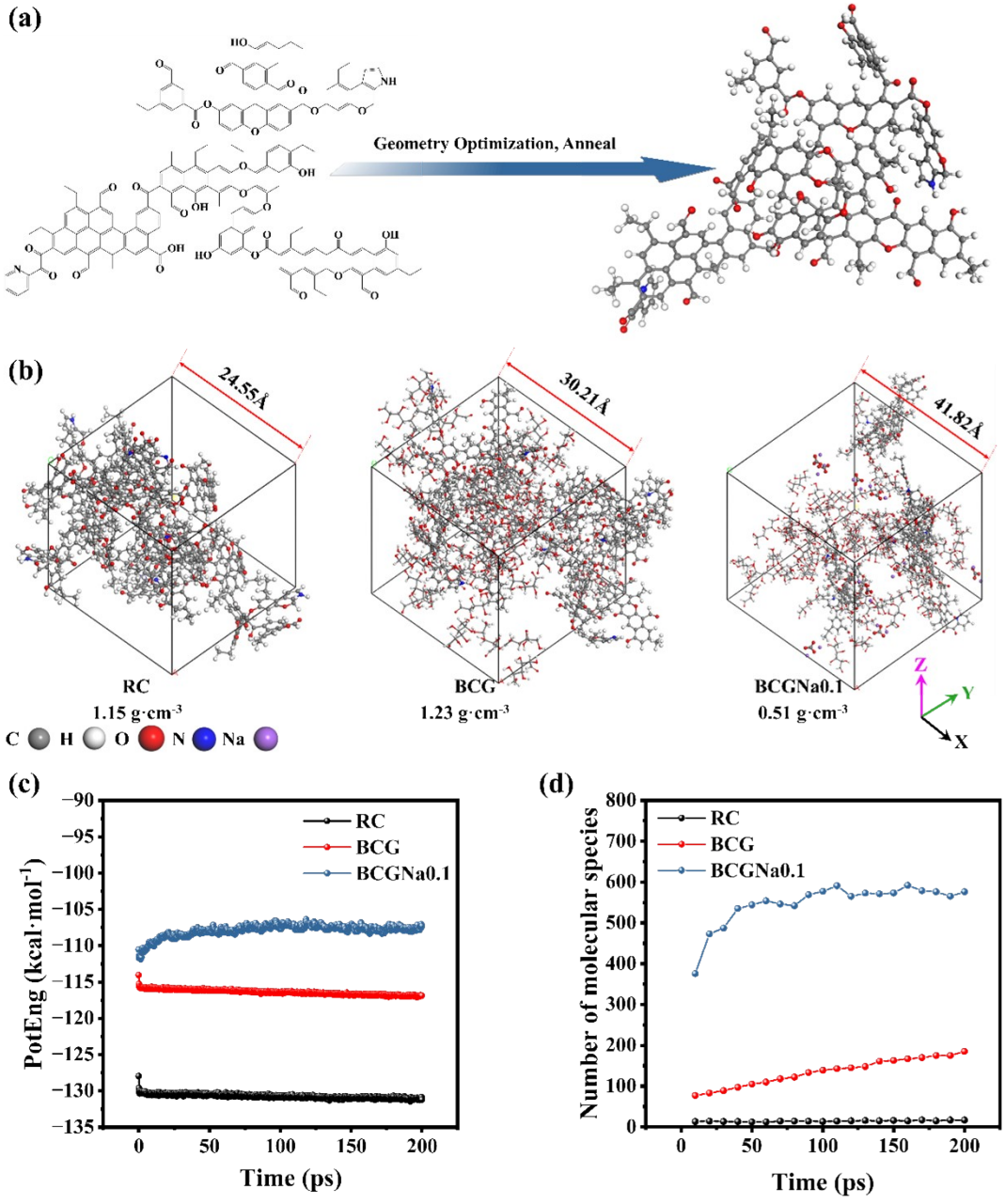


Figure S4 Structural evolution and pyrolysis behaviors of coal-based precursors. (a) Structural Optimization and Annealing Treatment: Coal Structure Before and After; (b) Optimized structural models of RC, BCG, and BCGNa0.1; (c) Evolution of

potential energy during ReaxFF-MD simulations; (d) Total number of pyrolysis fragments.

Figure S5 presents the TG-DTG curves of the three samples. The BCG sample exhibited multiple pyrolysis peaks near 200 °C, 300 °C, and 450 °C. The peaks at 200 °C and 300 °C are attributed to reactions between glucose and coal, leading to rapid volatile release and mass loss. Upon the addition of $Na_2CO_3$, the main decomposition peak shifted to 180 °C, indicating a catalytic effect on the pyrolysis process. Moreover, the DTG signal of the BCGNa0.1 sample was significantly intensified, confirming the acceleration of pyrolysis kinetics. The peak at 450 °C corresponds to the intrinsic decomposition of coal, primarily involving volatile release. Interestingly, the BCG sample showed reduced pyrolysis activity at this stage, suggesting that glucose facilitated the formation of cross-linked structures with coal, thereby enhancing the material’s thermal stability. These observations provide a basis for determining the appropriate pre-carbonization temperature.

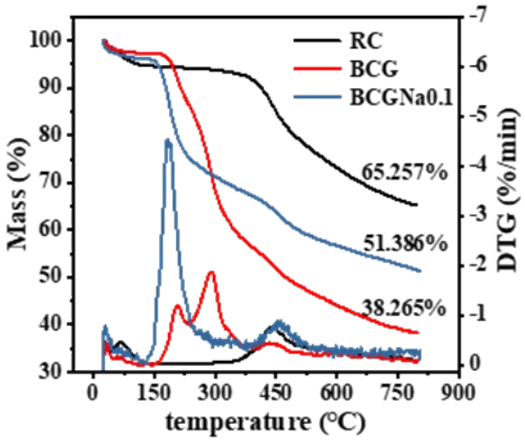


Figure S5 TG-DTG curves of RC, BCG, and BCGNa0.1

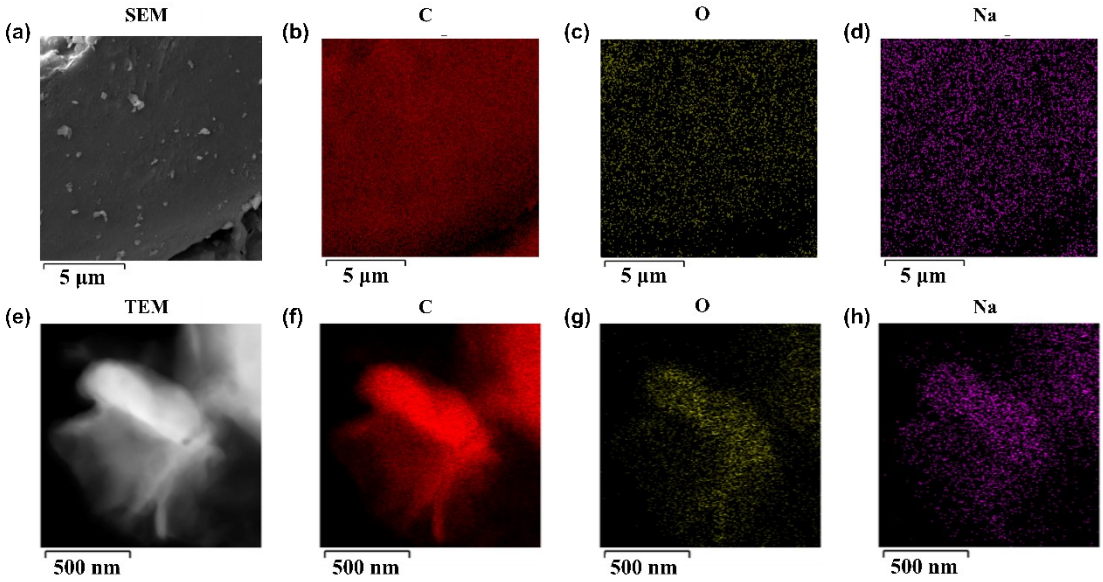


Figure S6 SEM-EDS and TEM-EDS of CGNa0.1

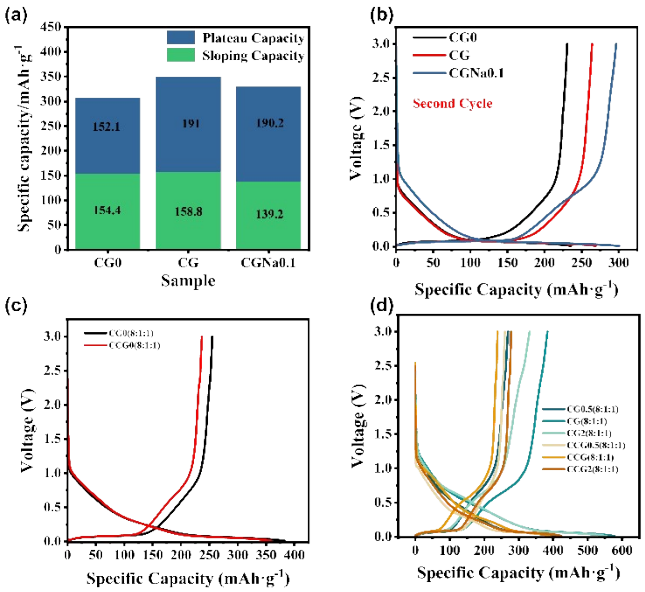


Figure S7 (a) Capacity contribution from the slope and plateau regions; (b) Second-cycle charge–discharge curve of CGNa0.1; (c-d) Comparison of charge–discharge profiles of CCGx, CGx, and CGNa0.1.

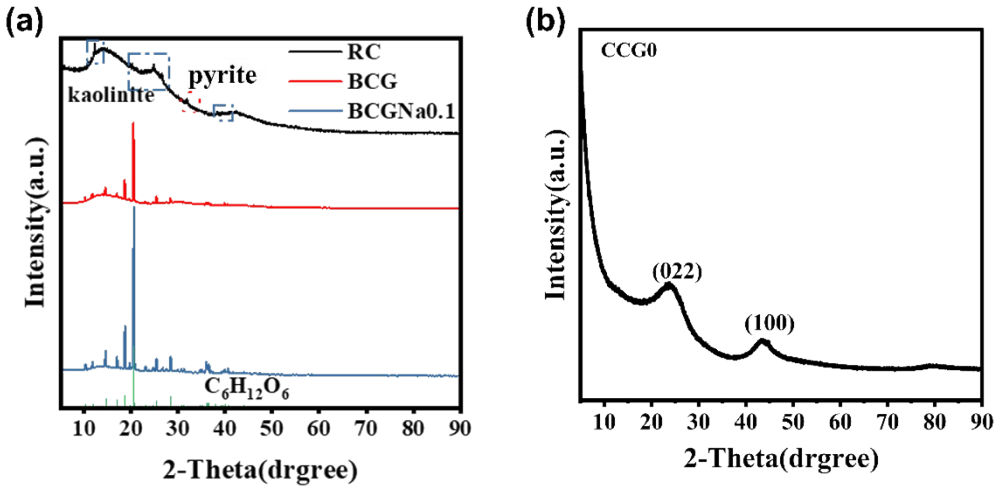


Figure S8 XRD patterns of (a) Pre-carbonization; (b) CCG0

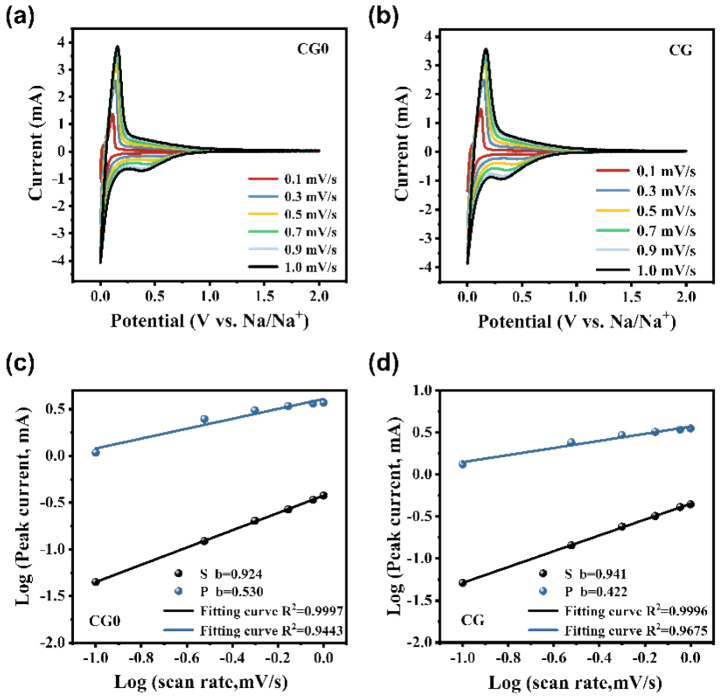


Figure S9 (a-b)CV curves of CG0, CG, and CGNa0.1 at different scan rates; (c-d) b-value fitting curves for corresponding redox peaks.

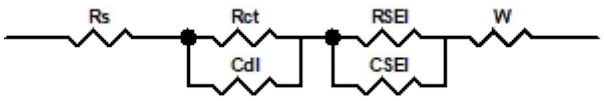


Figure S10 Equivalent Circuit of CGNa0.1

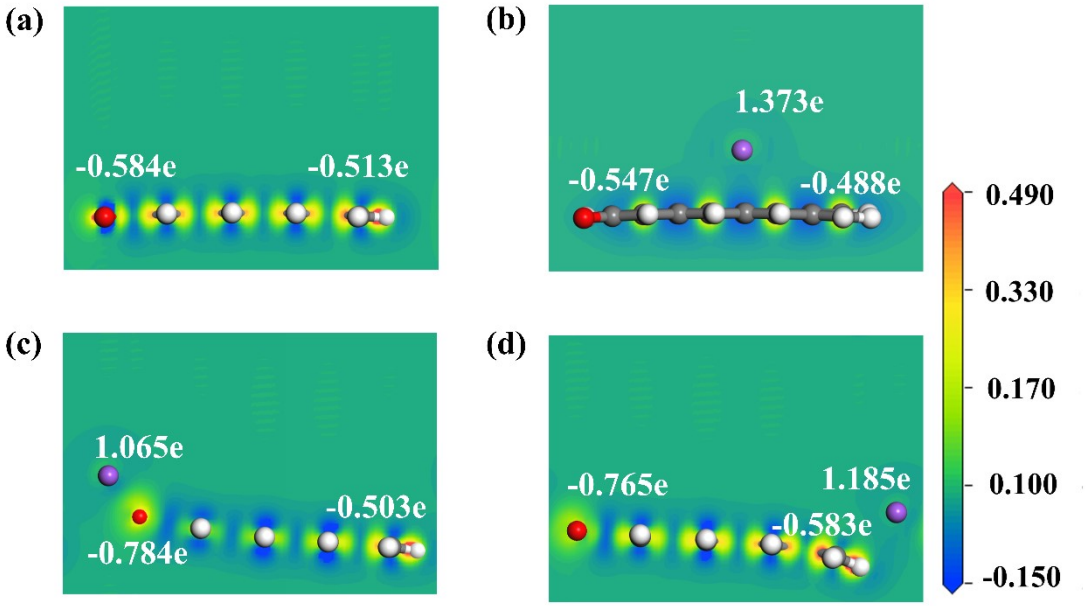


Figure S11 Electron density difference analysis of Na adsorption on carbon surfaces. (a) Charge distribution on carbon surfaces; (b) Na adsorption above the center of the carbon ring on carbon layer; (c) Na adsorption above the C---Na—O; (d) Na adsorption above the C—Na—O.

**Appendix 1：.in file**

```
variable a loop 2
log log.$a
variable T index 1573
units           real
atom_style    full
neighbor       2.0 bin
neigh_modify      every 1 delay 0 check no
read_data       CHONNa
pair_style     reaxff NULL
pair_coeff  * * ffield.reax.hns C H O N Na
neighbor        3 bin
neigh_modify    every 10 delay 0 check yes
#Temperature Initialization
velocity    all create $T 8888 loop all
timestep       0.1
thermo          2000
thermo_style custom step temp pe ke
thermo_modify     norm yes
fix 4 all nvt temp $T $T 100.0
fix 5 all qeq/reaxff 1 0.0 10.0 1.0e-6 reaxff
fix 6 all reaxff/species 1 1 100 species_${T}.out element C H O N Na
fix bondinfo all reaxff/bonds 1000 bonds.txt
dump  3 all atom 1000 dump_${T}.lammpstrj
run           2000000
```